PHASE SEPARATION

Partitioning of cancer therapeutics in nuclear condensates

Isaac A. Klein[1,2]*, Ann Boija[1]*, Lena K. Afeyan[1,3], Susana Wilson Hawken[1,3], Mengyang Fan[4,5], Alessandra Dall'Agnese[1], Ozgur Oksuz[1], Jonathan E. Henninger[1], Krishna Shrinivas[6,7], Benjamin R. Sabari[1], Ido Sagi[1], Victoria E. Clark[1,8], Jesse M. Platt[1,9], Mrityunjoy Kar[10], Patrick M. McCall[10,11,12], Alicia V. Zamudio[1,3], John C. Manteiga[1,3], Eliot L. Coffey[1,3], Charles H. Li[1,3], Nancy M. Hannett[1], Yang Eric Guo[1], Tim-Michael Decker[13], Tong Ihn Lee[1], Tinghu Zhang[4,5], Jing-Ke Weng[1,3], Dylan J. Taatjes[13], Arup Chakraborty[6,7,14,15,16,17,18], Phillip A. Sharp[3,18], Young Tae Chang[19], Anthony A. Hyman[11,20], Nathanael S. Gray[4,5], Richard A. Young[1,3]†

The nucleus contains diverse phase-separated condensates that compartmentalize and concentrate biomolecules with distinct physicochemical properties. Here, we investigated whether condensates concentrate small-molecule cancer therapeutics such that their pharmacodynamic properties are altered. We found that antineoplastic drugs become concentrated in specific protein condensates in vitro and that this occurs through physicochemical properties independent of the drug target. This behavior was also observed in tumor cells, where drug partitioning influenced drug activity. Altering the properties of the condensate was found to affect the concentration and activity of drugs. These results suggest that selective partitioning and concentration of small molecules within condensates contributes to drug pharmacodynamics and that further understanding of this phenomenon may facilitate advances in disease therapy.

T he five to 10 billion protein molecules of cells are compartmentalized into both membrane-bound and non–membrane-bound organelles (1–3). Many non–membrane-bound organelles are phase-separated biomolecular condensates with distinct physicochemical properties that can absorb and concentrate specific proteins and nucleic acids (4–17). We reasoned that selective condensate partitioning might also occur with small-molecule drugs with targets that occur within condensates (Fig. 1A), and that the therapeutic index and efficacy of such compounds might therefore relate to their ability to partition into condensates that harbor their target. To test this idea, we focused our study on a collection of nuclear condensates previously reported in cell lines, demonstrated that they all occur in normal human cells and in tumor cells, and then developed in vitro condensate droplet assays with key components of each of the nuclear condensates to enable testing of small molecules.

Nuclear condensates have been described in diverse cultured cell lines and contain one or more proteins that can serve both as markers of the condensate and as a scaffold for condensate formation in droplet assays in vitro (10–12, 18–31). Specifically, transcriptional condensates are marked by the condensate-forming proteins MED1 and BRD4 (10, 12, 19), splicing speckles by SRSF2 (11, 20), heterochromatin by HP1α (21, 22), and nucleoli by FIB1 and NPM1 (23–25) (fig. S1A). To determine whether such condensates can also be observed in the cells of healthy and malignant human tissue, we obtained biopsies of breast ductal epithelium, invasive ductal carcinoma, normal colon, and colon cancer (fig. S1, B and C). Immunofluorescence revealed nuclear bodies containing these marker proteins in both normal and transformed tissue (Fig. 1, B and C). There was a broad distribution of nuclear body sizes and numbers, as expected for dynamic biomolecular condensates, and no significant differences were observed between benign and malignant tissue (fig. S2, A to C). However, tumor cells acquire large superenhancers (SEs) at driver oncogenes (32) and these can form tumor-specific transcriptional condensates.

We developed an assay to model these nuclear condensates and study the behavior of small molecules within these droplets (Fig. 1D). We produced and purified recombinant, fluorescently labeled versions of MED1, BRD4, SRSF2, HP1α, FIB1, and NPM1 (fig. S3, A and B) and confirmed the ability of these proteins to form droplets in an in vitro assay (fig. S4, A and B). To investigate the partitioning behavior of small molecules, we added the dyes fluorescein (332 Da) and Hoechst (452 Da), as well as fluorescently labeled dextrans (4.4 kDa), to solutions containing each of the six protein condensates. The dyes and dextrans appeared to diffuse through all the condensates without substantial partitioning (Fig. 1E and figs. S5 and S6, A to D). Small-molecule drugs are generally smaller than 1 kDa, so these results suggested that small molecules can freely diffuse through these nuclear condensates unless there are factors other than size that influence partitioning.

We next sought to determine whether diverse clinically important drugs with targets that reside in nuclear condensates also exhibit free diffusion across these condensates or if they display a different behavior. Cisplatin and mitoxantrone, members of a class of antineoplastic compounds that modify DNA through platination or intercalation, can either be modified to have fluorescent properties (cisplatin) (33) or are already inherently fluorescent (mitoxantrone). When added to droplet formation buffer with purified MED1, BRD4, SRSF2, HP1α, FIB1, or NPM1, cisplatin was found to be selectively concentrated in MED1 droplets (Fig. 2A and fig. S7A), with a partition coefficient of up to 600 (fig. S8, A to C). Fluorescent modification of cisplatin did not appear to contribute to this behavior in vitro, because the modified drug could be chased out of the condensate with unmodified cisplatin, and an isomer of cisplatin did not exhibit the same behavior (fig. S7, B to D). Mitoxantrone was also concentrated in MED1 condensates, as well as in FIB1 and NPM1 condensates (Fig. 2B and fig. S7A). Consistent with these results, mitoxantrone is known to concentrate in the nucleolus, where FIB1 and NPM1 reside (34, 35). These results show that, in contrast to the dyes tested above, small-molecule drugs may concentrate in certain condensates even in the absence of the drug target.

We selected for further study antineoplastic drugs that target transcriptional regulators

[1]Whitehead Institute for Biomedical Research, Cambridge, MA 02142, USA. [2]Dana-Farber Cancer Institute, Harvard Medical School, Boston, MA 02215, USA. [3]Department of Biology, Massachusetts Institute of Technology, Cambridge, MA 02139, USA. [4]Department of Cancer Biology, Dana-Farber Cancer Institute, Boston, MA 02215, USA. [5]Department of Biological Chemistry and Molecular Pharmacology, Harvard Medical School, Boston, MA 02115, USA. [6]Department of Chemical Engineering, Massachusetts Institute of Technology, Cambridge, MA 02139, USA. [7]Institute for Medical Engineering and Science, Massachusetts Institute of Technology, Cambridge, MA 02139, USA. [8]Department of Neurosurgery, Massachusetts General Hospital and Harvard Medical School, Boston, MA 02114, USA. [9]Division of Gastroenterology, Department of Medicine, Massachusetts General Hospital, Boston, MA, 02114, USA. [10]Max Planck Institute for the Physics of Complex Systems, 01187 Dresden, Germany. [11]Max Planck Institute of Molecular Cell Biology and Genetics, 01307 Dresden, Germany. [12]Center for Systems Biology Dresden, 01307 Dresden, Germany. [13]Department of Biochemistry, University of Colorado, Boulder, CO 80303, USA. [14]Department of Physics, Massachusetts Institute of Technology, Cambridge, MA 02139, USA. [15]Department of Chemistry, Massachusetts Institute of Technology, Cambridge, MA 02139, USA. [16]Department of Biological Engineering, Massachusetts Institute of Technology, Cambridge, MA 02139, USA. [17]Ragon Institute of Massachusetts General Hospital, Massachusetts Institute of Technology and Harvard Medical School, Cambridge, MA 02139, USA. [18]Koch Institute for Integrative Cancer Research, Massachusetts Institute of Technology, Cambridge, MA 02139, USA. [19]Department of Chemistry, Pohang University of Science and Technology, and Center for Self-assembly and Complexity, Institute for Basic Science (IBS), Pohang 37673, Republic of Korea. [20]Cluster of Excellence Physics of Life, Technical University of Dresden, 01062 Dresden, Germany.
*These authors contributed equally to this work.
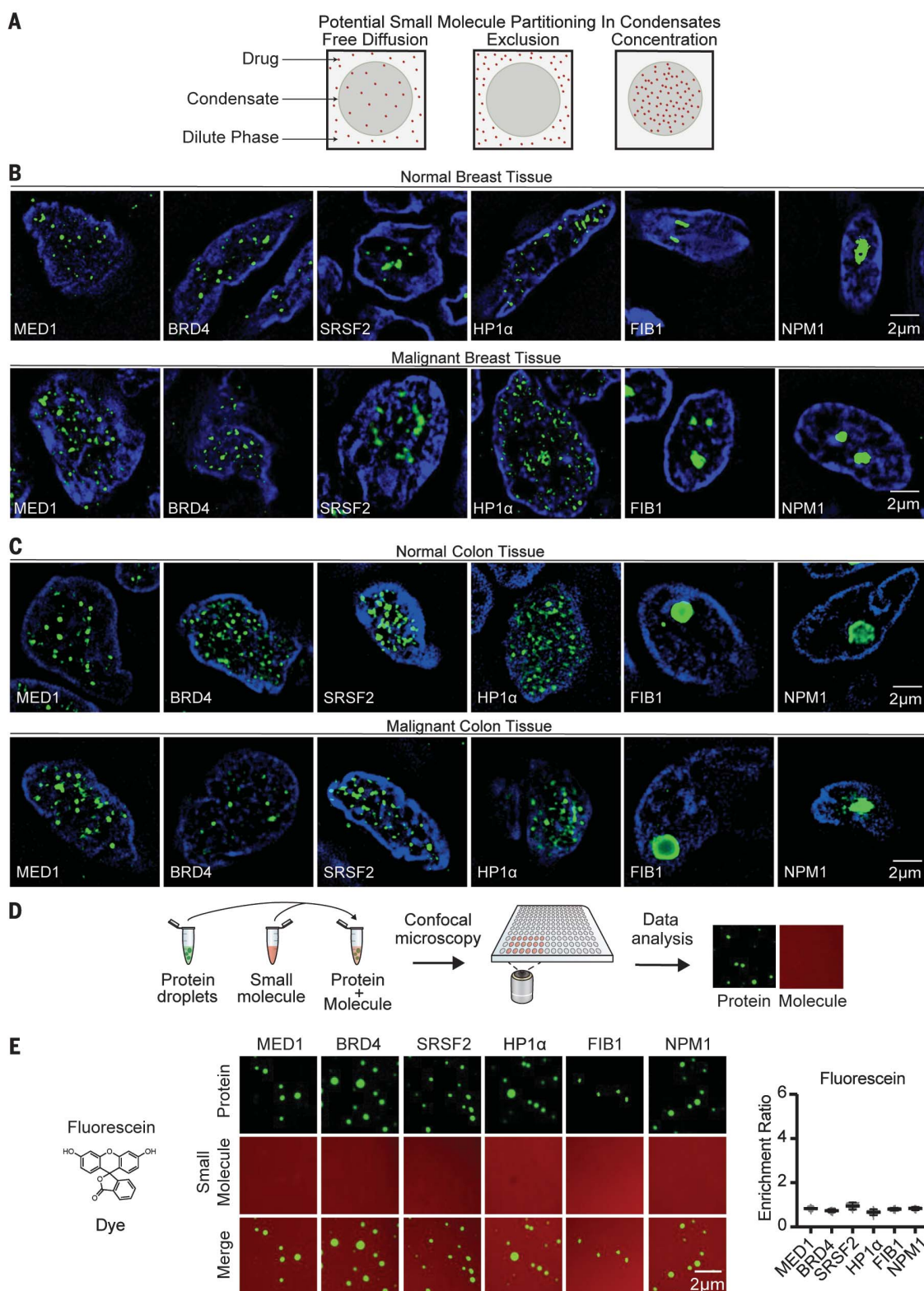†Corresponding author. Email: young@wi.mit.edu

Fig. 1. Nuclear condensates in human tissue and in vitro. (**A**) Model illustrating the potential behaviors of small molecules in nuclear condensates. (**B** and **C**) Immunofluorescence of scaffold proteins of various nuclear condensates in tissue biopsies from benign and malignant human breast tissue (B) and from benign and malignant colon tissue (C) in nuclei stained with Hoechst and imaged at 100× on a fluorescent confocal microscope (see also figs. S1 and S2). (**D**) Schematic of in vitro droplet formation assay to measure small-molecule partitioning into nuclear condensates. (**E**) In vitro droplet assay showing the behavior of fluorescein dye in the presence of six protein condensates formed in 125 mM NaCl and 10% PEG with 10 μM protein and 5 μM fluorescein imaged at 150× on a confocal fluorescent microscope (see also figs. S3 to S6). Quantification of enrichment of the drug is shown on the right. Error bars represent SEM.

expected to be contained within transcriptional condensates in cells. These targets include: (i) the estrogen receptor (ER), a transcription factor and nuclear hormone receptor; (ii) CDK7, a cyclin-dependent kinase that functions in transcription initiation and cell cycle control; and (iii) BRD4, a bromodomain protein and coactivator involved in oncogene regulation (fig. S9, A and B). To monitor drug behavior with a confocal fluorescent microscope, we used a fluorescent tamoxifen analog (FLTX1) that targets ER and modified fluorescent THZ1 and JQ1, which target CDK7 and BRD4, respectively (36, 37). FLTX1 and THZ1 concentrated preferentially in MED1 droplets (Fig. 2, C and D, and fig. S7A), and this behavior was not attributable to the fluorescent moiety (fig. S7, B and D). JQ1 concentration presented a different pattern, being concentrated in MED1, BRD4, and NPM1 droplets (Fig. 2E and fig. S7, A and B). Reinforcing these results, we found that the small molecules that concentrated in MED1 condensates were also concentrated in condensates formed from purified whole Mediator complexes (fig. S10A) and in MED1 condensates formed in an alternative crowding agent (fig. S11A). The targets of these three compounds (ERα, CDK7, and the bromodomains of BRD4) are not present in these in vitro condensates but are present in the SEs that form condensates with transcription factors and Mediator in vivo (10, 12, 38) (fig. S9, A and B), suggesting that the ability of some small molecules to concentrate preferentially in the same condensate as their protein target may contribute to the pharmacological properties of these drugs.

To gain additional insight into the nature of interactions governing small-molecule enrichment in condensates, we focused on the MED1-IDR condensate. Fluorescence recovery after photobleaching (FRAP) experiments showed that cisplatin molecules were highly mobile in this condensate (fig. S12, A and B), suggesting that the condensate produces a physicochemical environment that facilitates drug concentration in a state of high dynamic mobility. To gain insights into the chemical features of small molecules that may contribute to selective association with MED1 in condensates, we used a fluorescent boron-dipyrromethene (BODIPY) library of 81 compounds with various combinations of chemical side groups (fig. S13A). Molecules that contained aromatic rings were found to preferentially concentrate in MED1 condensates (figs. S13, A to D, and S14A). These data suggest that pi–pi or pi–cation interactions are among the physicochemical properties that favor small-molecule partitioning into MED1 condensates. Aromatic amino acids participate in pi–system interactions and are overrepresented in the MED1 IDR relative to the other condensate-forming proteins studied (fig. S3B). We generated a MED1 aromatic mutant protein (all 30 aromatic amino acids mutated to alanine) that retained the ability to form droplets in vitro, indicating that the aromatic amino acids are not required for droplet formation (fig. S14, B and C), but small-molecule probes containing aromatic rings and the polar molecule cisplatin no longer partitioned into condensates
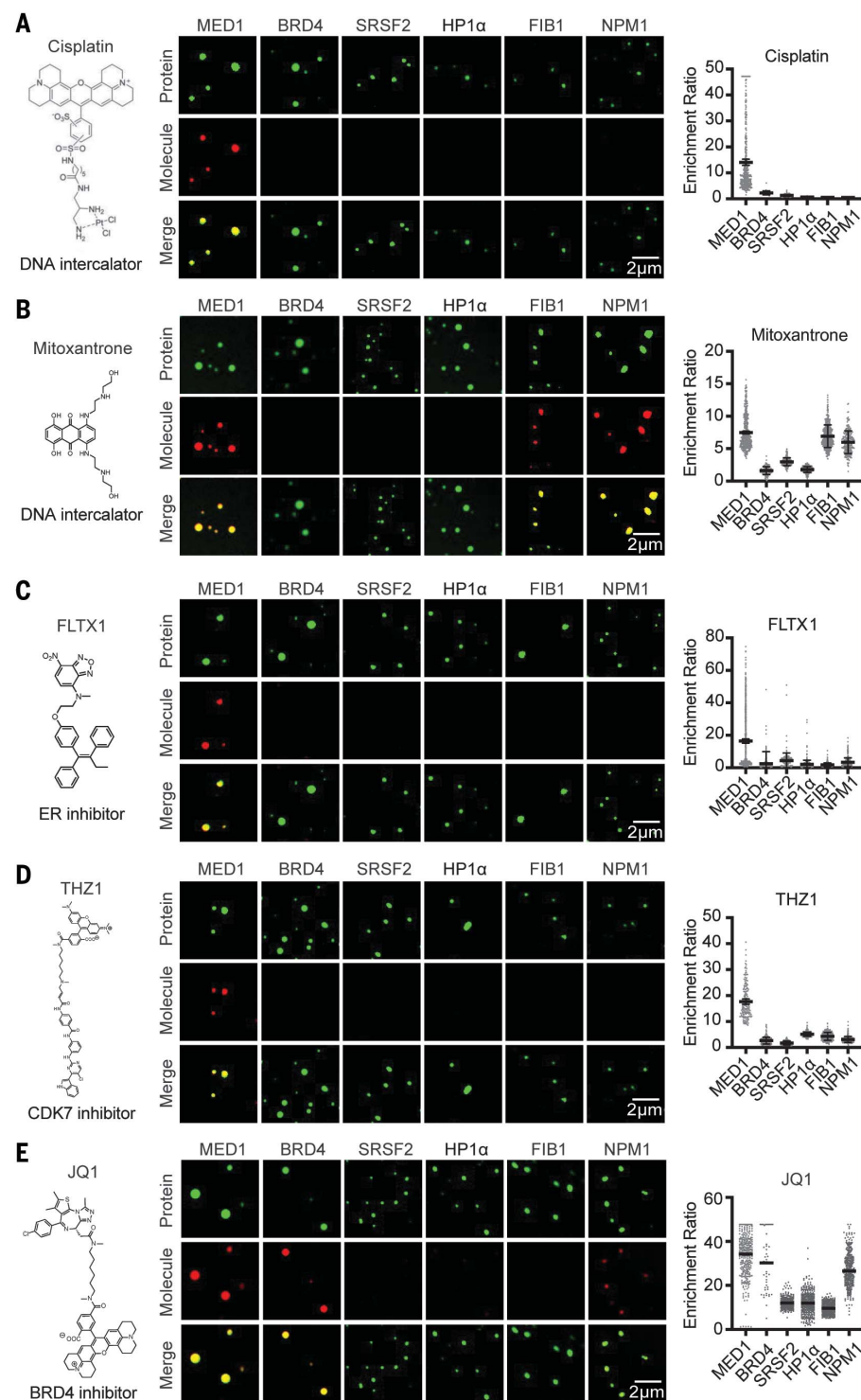

Fig. 2. Partitioning behavior of small-molecule drugs in nuclear condensates in a droplet assay.
Six nuclear condensates formed in 125 mM NaCl and 10% PEG with 10 μM protein treated with (**A**) 5μM cisplatin-TMR, (**B**) 50 μM mitoxantrone, (**C**) 100 μM FLTX1, (**D**) 5 μM THZ1-TMR, or (**E**) 1 μM JQ1-ROX imaged at 150× on a confocal fluorescent microscope (see also figs. S7 to S11). Quantification of enrichment of the drug within droplets is shown on the right of each panel. Error bars represent SEM (see also figs. S12 to S14).

**Fig. 3. Small-molecule concentration within condensates influences drug activity.** (**A**) In vitro droplet assay of MED1 and HP1α condensates formed in 125 mM NaCl and 10% PEG, 5 nM of 450-bp DNA, 10 μM MED1, and 5 μM cisplatin-TR imaged at 150× on a confocal fluorescent microscope (see also fig. S15). (**B**) Bioanalyzer tracings of DNA contained within either MED1 or HP1α droplets exposed to the indicated concentration of cisplatin. (**C**) (Top) Schematic of an assay to determine the location of platinated DNA relative to various nuclear condensates. (Bottom) Coimmunofluorescence of platinated DNA and the indicated protein in HCT116 cells treated with 50 μM cisplatin for 6 hours imaged at 100× on a confocal fluorescent microscope. Quantification of overlap is shown on the right. (**D**) (Top) Schematic of a live-cell condensate dissolution assay. (Bottom) HCT116 cells bearing endogenously mEGFP-tagged MED1, HP1α, or FIB1 treated with 50 μM cisplatin for 12 hours. Quantification of MED1, HP1α, or FIB1 condensate score is shown on the right. (**E**) MED1 ChIP-seq in HCT116 cells treated with vehicle or 50 μM cisplatin for 6 hours. (Left) Mean read density of MED1 at SEs and typical enhancers. Error bars represent minimum and maximum. (Right) Gene tracks of MED1 ChIP-Seq at the *MYC* SE and AQPEP typical enhancer. (**F**) Metaplot of cisplatin-DNA-Seq in cisplatin-treated HeLa cells comparing SEs and typical enhancers (*40*) (see also figs. S16 to S21).
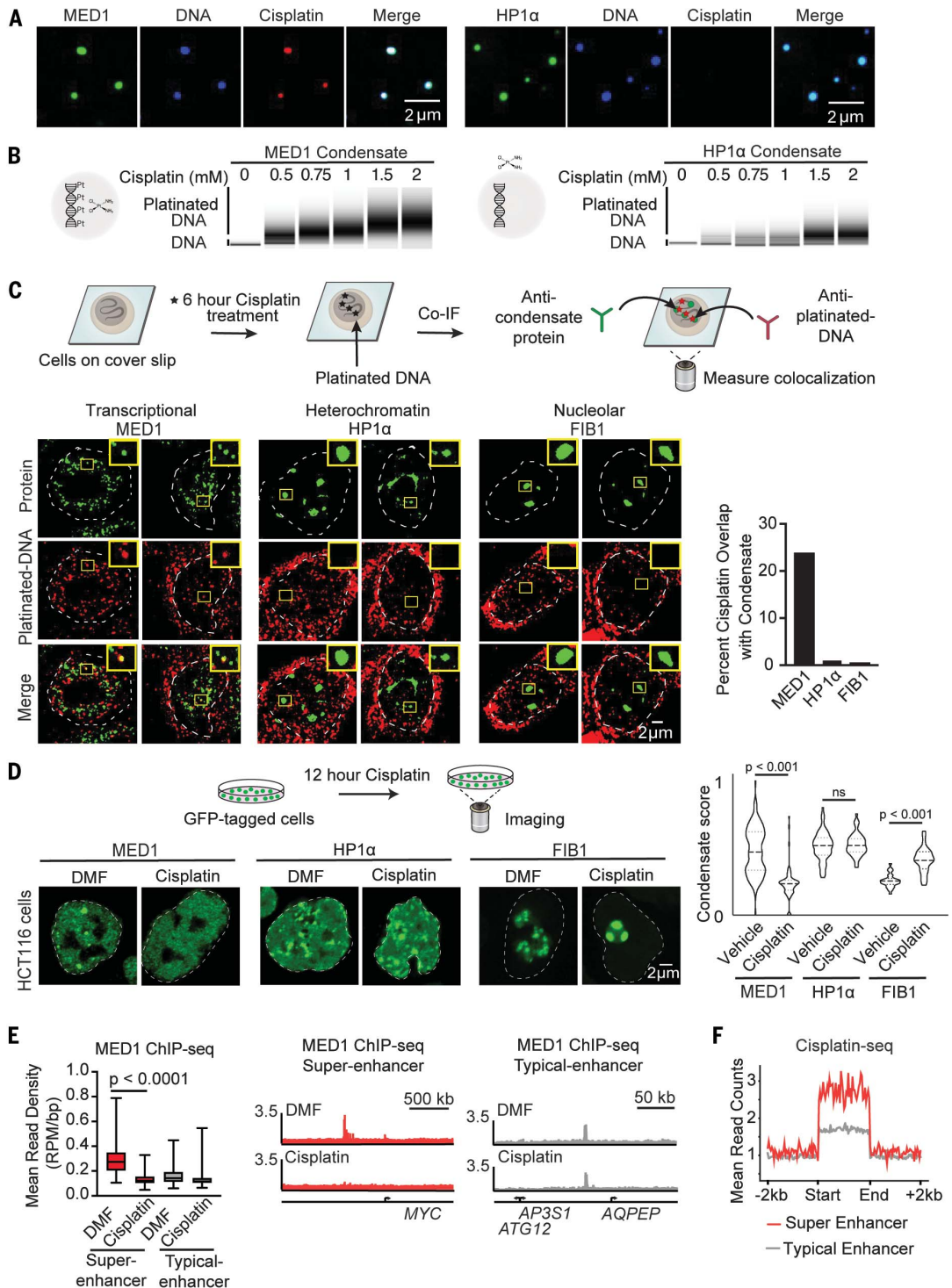
formed by the MED1 aromatic mutant protein (fig. S14, D to F). These results suggest that the aromatic residues of MED1 condensates contribute to the physicochemical properties that selectively concentrate these small molecules.

We anticipated that the ability of small molecules to concentrate in specific condensates would influence target engagement and thus drug pharmacodynamics. To investigate this, we took advantage of the ability of condensates to incorporate DNA (Fig. 3A and fig. S15A) and measured the relative efficiency of DNA platination by cisplatin in MED1 condensates, where cisplatin is concentrated, versus HP1α condensates, where cisplatin freely diffuses (Fig. 2A). DNA platination, visualized by size shift on a bioanalyzer, was more prevalent in MED1 condensates than in HP1α condensates (Fig. 3B), consistent with the expectation that elevated concentrations of cisplatin in the MED1 condensates yield enhanced target

engagement. If cisplatin becomes concentrated in Mediator condensates in cells, then we would expect that DNA colocalized within Mediator condensates would be preferentially platinated. To test this idea, we performed coimmunofluorescence in cisplatin-treated HCT116 colon cancer cells using an antibody that specifically recognizes platinated DNA (fig. S16A) (*39*), together with antibodies specific for MED1, HP1α, or FIB1. Consistent with

cisplatin's preference for MED1 condensates in vitro, we found that platinated DNA frequently colocalized with MED1 condensates but not with HP1α or FIB1 condensates (Fig. 3C). To determine whether the ability of cisplatin to engage DNA is dependent on the presence of a MED1 condensate, we treated cells with JQ1, which caused a loss of MED1 condensates (fig. S16B), and observed a concomitant reduction in platinated DNA at the

MYC oncogene (fig. S16, C and D). These results are consistent with the idea that the concentration of small molecules in specific condensates can influence the efficiency of target engagement.

In cells, the preferential modification of DNA in MED1-containing condensates might be expected to selectively disrupt these condensates with prolonged treatment. To test this, HCT116 colon cancer cells were engineered
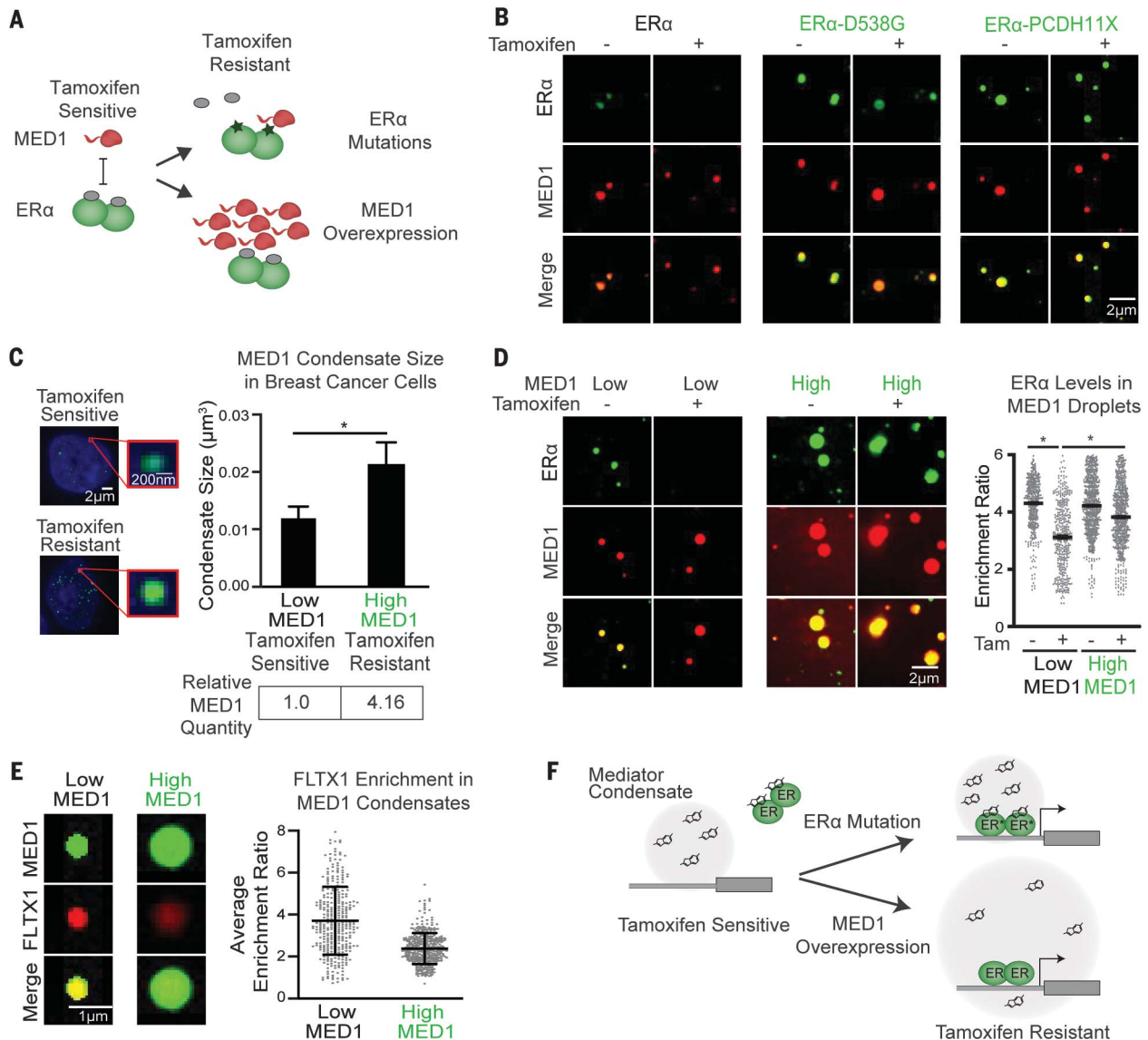
Fig. 4. Tamoxifen action and resistance in MED1 condensates. (**A**) Schematic showing tamoxifen resistance by ER mutation and MED1 overexpression in breast cancer. (**B**) In vitro droplet assay of the indicated form of GFP-tagged ER in the presence of estrogen with and without 100 μM tamoxifen. Droplets are formed in 125 mM NaCl and 10% PEG with a 10 μM concentration of each protein and 100 μM estrogen. (**C**) (Left) Immunofluorescence of MED1 in tamoxifen-sensitive (MCF7) and tamoxifen-resistant (TAMR7) ER⁺ breast cancer cell lines imaged at 100× on a confocal fluorescent microscope. (Top right) Quantification of MED1 condensate size in breast cancer cells. (Bottom right) Relative quantities of MED1 in the indicated breast cancer cell line by Western blot. Error bars represent SEM. (**D**) In vitro droplet assays of ER in the presence of 100 μM estrogen with and without 100 μM tamoxifen with either 5 μM (low) or 20 μM (high) MED1. Droplets are formed with 5 μM ER in 125 mM NaCl and 10% PEG and imaged at 150× on a confocal fluorescent microscope. Error bars represent SEM. (**E**) In vitro droplet assay with either 5 μM (low) or 20 μM (high) MED1 with 100 μM FLTX1 in 125 mM NaCl and 10% PEG. Error bars represent SD. (**F**) Models for tamoxifen resistance caused by altered drug affinity (through ER mutation) or concentration (through MED1 overexpression) (see also figs. S22 to S30).

to express green fluorescent protein (GFP)–tagged marker proteins for each of the six nuclear condensates (figs. S17, A to F, and S18, A and B). When exposed to cisplatin, a selective and progressive reduction in MED1 condensates was observed (Fig. 3D and figs. S19, A and B, and S20A). Consistent with this, cisplatin treatment led to a preferential loss of MED1 chromatin immunoprecipitation sequencing (ChIP-seq) signal at SEs (Fig. 3E and fig. S21A). Furthermore, high-throughput sequencing data from platinated-DNA pulldown (40) revealed that cisplatin-modified DNA preferentially occurs at SEs, where MED1 is concentrated (41) (Fig. 3F). These results are consistent with reports that cisplatin preferentially modifies transcribed genes (40, 42) and suggest that this effect is due to preferential condensate partitioning. Taken together, these results suggest a model in which cisplatin preferentially modifies SE DNA, which in turn leads to dissolution of these condensates. Previous studies have shown that diverse tumor cells become highly dependent on SE-driven oncogene expression (43–47), which might explain why platinum drugs, which are capable of general DNA modification, are effective therapeutics in diverse cancers (48).

We explored the behavior of another clinically important antineoplastic drug, tamoxifen, to assess whether its drug response and resistance were associated with partitioning in condensates (Fig. 4A). ERα incorporates into MED1 condensates in an estrogen-dependent manner in vitro (12); droplet assays confirmed this and revealed that the addition of tamoxifen leads to eviction of ERα from the MED1 condensates (Fig. 4B). We further investigated the effects of estrogen and tamoxifen on MED1 condensates in breast cancer cells, focusing on the *MYC* oncogene because of its prominent oncogenic role and responsiveness to estrogen (49). MED1 condensates were observed on the *MYC* oncogene in the ER⁺ breast cancer cell line MCF7 (figs. S9A and S22, A to D). DNA fluorescence in situ hybridization with MED1 immunofluorescence revealed that estrogen enhances the formation of MED1 condensates at the *MYC* oncogene and that tamoxifen treatment reduces it (fig. S23, A and B). Artificial MED1 condensates without ER concentrated FLTX1 at the site of the condensate (fig. S24A), indicating that ER is not required for the partitioning of FLTX1 into MED1 condensates in cells. These results are consistent with the model that ERα interacts with MED1 condensates in an estrogen-dependent, tamoxifen-sensitive manner to drive oncogene expression in breast cancer cells.

The mechanisms that produce drug resistance can provide clues to drug activity in the clinical setting. Endocrine therapy and tamoxifen resistance are an enduring clinical challenge and are associated with multiple mechanisms, including ERα mutation and MED1 overexpression (Fig. 4A and fig. S25) (50–54). To investigate whether ERα mutations alter ERα behavior in condensates, we produced four patient-derived ERα mutant proteins and tested their partitioning in the presence of tamoxifen. In contrast to wild-type ERα, condensates composed of patient-derived ERα mutants and MED1 were not disrupted upon tamoxifen treatment (Fig. 4B and fig. S26, A and B). The ERα point mutations reduce the affinity for tamoxifen by ~10-fold (51), indicating that the drug concentration in the droplet is inadequate to evict these ER mutant proteins when this affinity is reduced.

MED1 overexpression is associated with tamoxifen resistance and poor prognosis in breast cancer (50), but it is not clear why overexpression of one subunit of the Mediator complex produces resistance. We considered the possibility that overexpressed MED1 is incorporated into transcriptional condensates, which contain clusters of Mediator molecules (38), thereby expanding their volumes and diluting the available tamoxifen (fig. S27A). We found that the tamoxifen-resistant breast cancer cell line TAMR7 (55), which was derived from the tamoxifen-sensitive cell line MCF7, produced fourfold elevated levels of the MED1 protein (fig. S27B). The volume of MED1-containing condensates was twofold larger in these cells (Fig. 4C and fig. S27C). When modeled in an in vitro droplet assay, we found that a fourfold increase in MED1 levels led to a commensurate increase in droplet size (fig. S28, A and B). Furthermore, we found that 100 μM tamoxifen prevented ERα incorporation into MED1 condensates (Fig. 4, B and D), but was much less effective in preventing ERα incorporation into the larger MED1 condensates produced with higher MED1 levels (Fig. 4D). To confirm that the levels of tamoxifen in the larger droplets are more dilute, we measured the enrichment of the fluorescent tamoxifen analog FLTX1 in MED1 droplets and found that the larger condensates had lower concentrations of the drug (Fig. 4E). These results were mirrored in cells, where a collection of tethered ERα molecules formed a MED1 condensate that was eliminated by tamoxifen, but when MED1 was overexpressed, tamoxifen was unable to dissociate the ERα-MED1 condensate (fig. S29A). Similarly, knockdown of MED1 in tamoxifen-resistant breast cancer cells sensitizes cells to tamoxifen (50, 54). These results support a model of tamoxifen resistance where MED1 overexpression causes the formation of larger transcriptional condensates in which tamoxifen is diluted and is thereby less effective at dissociating ER from the condensate (Fig. 4F).

Our results show that drugs partition selectively into condensates, that this can occur through physicochemical properties that exist independently of their molecular targets, and that cells can develop resistance to drugs through condensate-altering mechanisms. This may explain the surprising observation that inhibition of global gene regulators such as BRD4 or CDK7 can have selective effects on oncogenes that have acquired large SEs (45); selective partitioning of inhibitors such as JQ1 and THZ1 into SE condensates will preferentially disrupt transcription at those loci. These results also have implications for the future development of efficacious disease therapeutics; effective target engagement will depend on measurable factors such as drug partitioning in condensates (fig. S30, A to D). Condensate assays of the type described here may thus help to optimize condensate partitioning, target engagement, and the therapeutic index of small-molecule drugs.

REFERENCES AND NOTES

1. Y. Shin, C. P. Brangwynne, *Science* **357**, eaaf4382 (2017).
2. S. F. Banani, H. O. Lee, A. A. Hyman, M. K. Rosen, *Nat. Rev. Mol. Cell Biol.* **18**, 285–298 (2017).
3. A. A. Hyman, C. A. Weber, F. Jülicher, *Annu. Rev. Cell Dev. Biol.* **30**, 39–58 (2014).
4. R. J. Ries *et al.*, *Nature* **571**, 424–428 (2019).
5. E. M. Langdon, A. S. Gladfelter, *Annu. Rev. Microbiol.* **72**, 255–271 (2018).
6. E. M. Langdon *et al.*, *Science* **360**, 922–927 (2018).
7. M.-T. Wei, Y.-C. Chang, S. F. Shimobayashi, Y. Shin, C. P. Brangwynne, Nucleated transcriptional condensates amplify gene expression. bioRxiv 737387 [Preprint]. 21 August 2019; https://doi.org/10.1101/737387.
8. T. J. J. Nott *et al.*, *Mol. Cell* **57**, 936–947 (2015).
9. T. J. Nott, T. D. Craggs, A. J. Baldwin, *Nat. Chem.* **8**, 569–575 (2016).
10. B. R. Sabari *et al.*, *Science* **361**, eaar3958 (2018).
11. Y. E. Guo *et al.*, *Nature* **572**, 543–548 (2019).
12. A. Boija *et al.*, *Cell* **175**, 1842–1855.e16 (2018).
13. J. J. Bouchard *et al.*, *Mol. Cell* **72**, 19–36.e8 (2018).
14. K. Shrinivas *et al.*, *Mol. Cell* **75**, 549–561.e7 (2019).
15. E. P. Bentley, B. B. Frey, A. A. Deniz, *Chemistry* **25**, 5600–5610 (2019).
16. M. Boehning *et al.*, *Nat. Struct. Mol. Biol.* **25**, 833–840 (2018).
17. P. Cramer, *Nature* **573**, 45–54 (2019).
18. S. Alberti *et al.*, *J. Mol. Biol.* **430**, 4806–4820 (2018).
19. D. Hnisz, K. Shrinivas, R. A. Young, A. K. Chakraborty, P. A. Sharp, *Cell* **169**, 13–23 (2017).
20. Y. Chen, A. S. Belmont, *Curr. Opin. Genet. Dev.* **55**, 91–99 (2019).
21. A. G. Larson *et al.*, *Nature* **547**, 236–240 (2017).
22. A. R. Strom *et al.*, *Nature* **547**, 241–245 (2017).
23. M. Feric *et al.*, *Cell* **165**, 1686–1697 (2016).
24. D. M. Mitrea *et al.*, *eLife* **5**, e13571 (2016).
25. D. M. Mitrea *et al.*, *Nat. Commun.* **9**, 842 (2018).
26. S. F. Banani *et al.*, *Cell* **166**, 651–663 (2016).
27. A. Patel *et al.*, *Cell* **162**, 1066–1077 (2015).
28. S. Alberti, *J. Cell Sci.* **130**, 2789–2796 (2017).
29. A. E. Posey, A. S. Holehouse, R. V. Pappu, "Chapter one - phase separation of intrinsically disordered proteins," in *Methods in Enzymology* (Elsevier, 2018), vol. 611, pp. 1–30.
30. V. N. Uversky, *Curr. Opin. Struct. Biol.* **44**, 18–30 (2017).
31. Y. S. Mao, B. Zhang, D. L. Spector, *Trends Genet.* **27**, 295–306 (2011).
32. D. Hnisz *et al.*, *Cell* **155**, 934–947 (2013).
33. Y. H. Chu *et al.*, *Mol. Pharm.* **13**, 2677–2682 (2016).
34. J. Vibet *et al.*, *Drug Metab. Dispos.* **35**, 822–828 (2007).
35. P. J. Smith, H. R. Sykes, M. E. Fox, I. J. Furlong, *Cancer Res.* **52**, 4000–4008 (1992).
36. N. Kwiatkowski *et al.*, *Nature* **511**, 616–620 (2014).
37. J. Marrero-Alonso *et al.*, *Eur. J. Pharm. Biopharm.* **85** (3 Pt B), 898–910 (2013).
38. W.-K. Cho *et al.*, *Science* **361**, 412–415 (2018).

39. M. J. Tilby et al., Cancer Res. **51**, 123–129 (1991).
40. X. Shu, X. Xiong, J. Song, C. He, C. Yi, Angew. Chem. Int. Ed. **55**, 14246–14249 (2016).
41. W. A. Whyte et al., Cell **153**, 307–319 (2013).
42. X. Rovira-Clave et al., Subcellular localization of drug distribution by super-resolution ion beam imaging. bioRxiv 557603 [Preprint]. 22 February 2019; https://doi.org/10.1101/557603.
43. Y. Wang et al., Cell **163**, 174–186 (2015).
44. M. R. Mansour et al., Science **346**, 1373–1377 (2014).
45. J. E. Bradner, D. Hnisz, R. A. Young, Cell **168**, 629–643 (2017).
46. J. Lovén et al., Cell **153**, 320–334 (2013).
47. Z. Nie et al., Cell **151**, 68–79 (2012).
48. S. Dasari, P. B. Tchounwou, Eur. J. Pharmacol. **740**, 364–378 (2014).
49. D. Dubik, T. C. Dembinski, R. P. C. Shiu, Cancer Res. **47**, 6517–6521 (1987).
50. A. Nagalingam et al., Carcinogenesis **33**, 918–930 (2012).
51. S. W. Fanning et al., eLife **5**, e12792 (2016).
52. C. S. Ross-Innes et al., Nature **481**, 389–393 (2012).
53. M. Murtaza et al., Nature **497**, 108–112 (2013).
54. J. Cui et al., Cancer Res. **72**, 5625–5634 (2012).
55. S. Hole et al., Int. J. Oncol. **46**, 1481–1490 (2015).

SUPPLEMENTARY MATERIALS

science.sciencemag.org/content/368/6497/1386/suppl/DC1
Materials and Methods
Figs. S1 to S30
References (56–68)
MDAR Reproducibility Checklist

View/request a protocol for this paper from Bio-protocol.

Science

Partitioning of cancer therapeutics in nuclear condensates

Isaac A. Klein, Ann Boija, Lena K. Afeyan, Susana Wilson Hawken, Mengyang Fan, Alessandra Dall'Agnese, Ozgur Oksuz, Jonathan E. Henninger, Krishna Shrinivas, Benjamin R. Sabari, Ido Sagi, Victoria E. Clark, Jesse M. Platt, Mrityunjoy Kar, Patrick M. McCall, Alicia V. Zamudio, John C. Manteiga, Eliot L. Coffey, Charles H. Li, Nancy M. Hannett, Yang Eric Guo, Tim-Michael Decker, Tong Ihn Lee, Tinghu Zhang, Jing-Ke Weng, Dylan J. Taatjes, Arup Chakraborty, Phillip A. Sharp, Young Tae Chang, Anthony A. Hyman, Nathanael S. Gray and Richard A. Young

Drug partitioning in nuclear condensates

There is increasing interest in the function of phase-separated biomolecular condensates in cells because of their distinct properties and expanding roles in important biological processes. Klein *et al.* considered the fate of small-molecule therapeutics in the context of nuclear condensates (see the Perspective by Viny and Levine). They show that certain antineoplastic drugs have physicochemical properties that cause them to concentrate preferentially in condensates, both in vitro and in cancer cells. This property influences drug activity, and protein mutations that alter condensate formation can lead to drug resistance. Optimizing condensate partitioning may be valuable in developing improved therapeutics.

Science, this issue p. 1386; see also p. 1314

ARTICLE TOOLS	http://science.sciencemag.org/content/368/6497/1386
SUPPLEMENTARY MATERIALS	http://science.sciencemag.org/content/suppl/2020/06/17/368.6497.1386.DC1
RELATED CONTENT	http://science.sciencemag.org/content/sci/368/6497/1314.full
REFERENCES	This article cites 62 articles, 12 of which you can access for free http://science.sciencemag.org/content/368/6497/1386#BIBL
PERMISSIONS	http://www.sciencemag.org/help/reprints-and-permissions

Use of this article is subject to the Terms of Service